Figure 3. Increase of peak current from **1d** due to NADH or ascorbate using differential pulse voltammetry. [**1d**] = 7 × 10⁻⁵ M, ν = 10 mV s⁻¹, modulation amplitude = 50 mV. (O) Increase of first peak current due to addition of ascorbate. (●) Increase of second peak current due to addition of NADH.

equivalent occurs from NADH to **2**[9] (see the transition state shown below). This mechanism accounts for the high reactivity of

1a–f
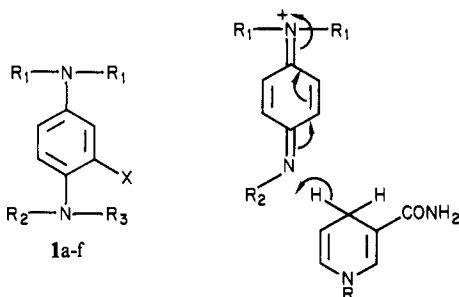
oxidized diamines in that iminium ions are known to be better hydride acceptors than ketones, and the mechanism has analogy in flavin oxidation of NADH. Most importantly, it accounts for the lack of catalysis from **1d**. **1d** has electrochemistry different from the other diamines discussed here, because it cannot lose an amino proton upon oxidation. At the first oxidation peak (see Figure 2a), only one electron is transferred forming **1d⁺·**. Because hydride addition on nitrogen would require that nitrogen expand its octet, **1d⁺·** is not a good hydride acceptor. It will be noted that **1d²⁺** could accept hydride, and, indeed, it should be an excellent NADH oxidant.

Ascorbic acid oxidation on carbon is very similar to NADH oxidation in that it has a large activation energy.[10] The cyclic voltammogram shows a difficult to reproduce, anodic peak at 0.4 V (Figure 1d). Several reports of the catalysis of this process have appeared,[2,11] and catalysis can also be achieved by using diamine **1a** (Figure 1e).[12] More interestingly, however, **1d** also gives good catalysis (Figure 2c).

These observations lead us to propose that an electroanalytical discrimination between NADH and ascorbate could be made by using **1d** or a similar catalyst. Because these two biological

reductants often coexist, the analytical problem is of some interest. We have discovered that **1d** can, indeed, provide separate electrochemical responses for NADH and ascorbate. The voltammogram of **1d** at pH 7.0 shows two anodic peaks, the first reversible and the second irreversible. *Ascorbic acid is catalyzed at the first peak and NADH at the second oxidation peak.*

In Figure 3 are shown the results of differential pulse voltammetry studies on NADH and ascorbate[13] by using 0.07 mM **1d** as a catalyst. For analyte concentrations less than 0.7 mM the first peak current responds linearly to ascorbate concentration and the second peak current responds linearly to NADH concentration. The mechanistic concept underlying these results should provide a guide, and more extensive studies with **1d** and other catalysts, therefore, may reveal a useful analytical method. Although differential pulse voltammetry is widely appreciated as a technique for mixture analysis, it has not, to our knowledge, been used in the presence of catalysts. The combination seems attractive and worthy of further exploration. The unexpected observation of catalysis of NADH oxidation from a chemically irreversible couple also deserves, and will receive, further study.

(13) Differential pulse polarograms of nicotinamide and ascorbic acid have been published: Lindquist, J.; Farroha, S. M. *Analyst (London)* **1975**, *100*, 377.

Reactivity of the [(η⁵-C₅H₅)Ti(Mo₅O₁₈)]³⁻ Anion: Synthesis and Structure of MoO₂Cl⁺ and Mn(CO)₃⁺ Adducts

V. W. Day,*[†‡§] M. F. Fredrich,[†] and M. R. Thompson[†]

*Department of Chemistry, University of Nebraska
Lincoln, Nebraska 68588
and Crystalytics Company
Lincoln, Nebraska 68501*

W. G. Klemperer,*[§] R.-S. Liu, and W. Shum

*Department of Chemistry, Columbia University
New York, New York 10027*

*Received January 12, 1981
Revised Manuscript Received April 20, 1981*

The [(η⁵-C₅H₅)Ti(Mo₅O₁₈)]³⁻ anion[1,2] (**1**) (see Figure 1) is surprisingly unstable relative to the VMo₅O₁₉³⁻ anion[2,3] which is closely related structurally by replacement of its [OVⱽ]³⁺ vanadyl group by a [(η⁵-C₅H₅)Tiᴵⱽ]³⁺ unit. The VMo₅O₁₉³⁻ anion is stable toward moisture and elevated temperature (80 °C) in CH₃CN whereas anion **1** decomposes rapidly under the same conditions. We have therefore examined the structure of anion **1** and its reactivity toward electrophiles in order to better understand the origin of this instability and utilize its reactivity to synthesize new types of polyoxoanion supported organometallic complexes. We report here preliminary results of these studies, which include (a) the first X-ray crystallographic structure determinations of polyoxoanion supported organometallic complexes to be reported in the

(9) In addition to iminium ions, e.g., **2**, there are three other oxidants which could be involved in the NADH reaction. They are diamine cation radicals, diamine dications, e.g., **1**, minus two electrons, and diamine, e.g., **2a**, minus a proton. The latter is improbable on the basis of the k_{rel} of **1a–c**. The cation radical and dication are more probable, but the k_{rel} of **1a–c** compared to **1d** supports iminium ions as the key oxidants. This problem will be resolved in a future publication.

(10) The electrochemistry of ascorbic acid has received continued attention, using various techniques and materials. See, for example: Pachla, L. A.; Kissinger, P. T. *Anal. Chem.* **1976**, *48*, 364. Perone, S.; Kretlow, W. J. *Ibid.* **1966**, *38*, 1763.

(11) Cheng, H.-Y.; Strope, E.; Adams, R. N. *Anal. Chem.* **1979**, *51*, 2243. Dautartis, M.; Evans, J. F. *J. Electroanal. Chem.* **1980**, *109*, 301. Evans, J. F.; Kuwana, T.; Henne, M. T.; Royer, G. P. *Ibid.* **1977**, *80*, 409.

(12) Ascorbic acid shows very large and irreproducible catalytic waves on the first sweep. Data were, therefore, taken on later cycles.

[†] University of Nebraska.
[‡] Crystalytics Company.
[§] Camille and Henry Dreyfus Teacher–Scholar.

(1) Unless otherwise specified, the (n-C₄H₉)₄N⁺ ion was employed as a countercation for all anions discussed in this communication.

(2) Klemperer, W. G.; Shum, W. *J. Chem. Soc., Chem. Commun.* **1979**, 60.

(3) Filowitz, M.; Ho, R. K. C.; Klemperer, W. G.; Shum, W. *Inorg. Chem.* **1979**, *18*, 93.
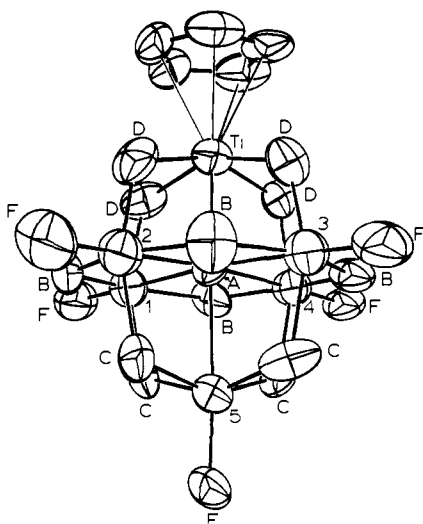
Figure 1. ORTEP drawing of the nonhydrogen atoms in the $[(\eta^5\text{-}C_5H_5)Ti(Mo_5O_{18})]^{3-}$ anion (**1**), as observed in single crystals of its $(n\text{-}C_4H_9)_4N^+$ salt. All atoms are represented by thermal vibration ellipsoids drawn to encompass 50% of the electron density. Molybdenum atoms are labeled with numbers and the 18 oxygen atoms labeled according to the following scheme: A for the single six-coordinated oxygen, B, C, or D for the 12 doubly bridging oxygens, and E and F for the 5 terminally bonded oxygen atoms. Carbon atoms of the $\eta^5\text{-}C_5H_5$ ring are not labeled. Bond lengths, averaged when appropriate in accord with idealized C_{4v} symmetry (the girdle molybdenums $Mo_1\text{-}Mo_4$ are designated Mo_g), are $Mo_5\text{-}O_E$ 1.72 (2), $Mo_g\text{-}O_F$ 1.69 (2,1,2,4),[13] $Mo_g\text{-}O_B$ 1.96 (2,4,6,8), $Mo_5\text{-}O_C$ 1.94 (2,2,3,4), $Mo_g\text{-}O_C$ 1.92 (2,1,2,4), $Mo_g\text{-}O_D$ 1.82 (2,1,2,4), $Ti\text{-}O_D$ 2.00 (2,2,4,4), $Mo_g\text{-}O_A$ 2.33 (2,2,2,4), $Mo_5\text{-}O_A$ 2.43 (2), $Ti\text{-}O_A$ 2.17 (2), Ti–C 2.45 (3,2,4,5), (cyclopentadienyl) C–C 1.41 (5,3,8,5) Å.
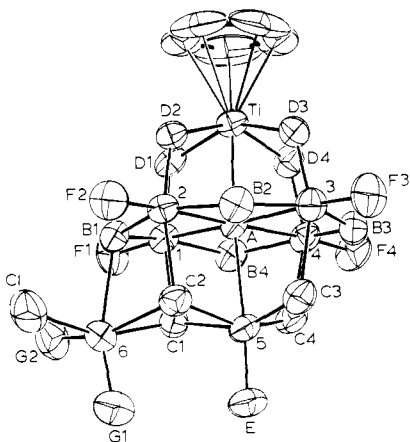

Figure 2. ORTEP drawing of the nonhydrogen atoms in the $[(\eta^5\text{-}C_5H_5)Ti(Mo_5O_{18})MoO_2Cl]^{2-}$ anion (**2**) as observed in single crystals of its $(n\text{-}C_4H_9)_4N^+$ salt. All atoms are represented by thermal vibration ellipsoids drawn to encompass 50% of the electron density. The labeling scheme employed for molybdenum and oxygen atoms is based on that used in Figure 1. The unique chlorine atom bonded to Mo_6 is labeled Cl. Carbon atoms in the $\eta^5\text{-}C_5H_5$ ring are not labeled. Bond lengths not given in the text, averaged in accord with approximate structural equivalence whenever possible, include $Mo_g\text{-}O_F$ 1.675 (9,2,5,4),[13] $Mo_5\text{-}O_E$ 1.675 (9), $Mo_5\text{-}O_{C3}$ 1.831 (8,11,11,2), $Mo_g\text{-}O_{C3}$ 2.027 (10,17,17,2), $Mo_g\text{-}O_A$ 2.312 (7,15,30,4), $Mo_5\text{-}O_A$ 2.402 (8), $Mo_g\text{-}O_D$ 1.787 (9,3,6,4), $Ti\text{-}O_D$ 1.996 (8,5,9,4), $Ti\text{-}C$ 2.365 (18,8,14,5), $Ti\text{-}O_A$ 2.343 (8), $Mo_6\text{-}O_{B1}$ 2.274 (8), $Mo_6\text{-}O_{G1}$ 1.679 (10), $Mo_6\text{-}O_{G2}$ 1.696 (10), $Mo_6\text{-}Cl$, 2.353 (4), (cyclopentadienyl) C–C 1.33 (3,3,5,5) Å.

literature, those of anion **1** and the $[(\eta^5\text{-}C_5H_5)Ti(Mo_5O_{18})\text{-}MoO_2Cl]^{2-}$ anion, and (b) the synthesis and structure of the first bifunctional polyoxoanion supported organometallic, the hydrocarbyl–carbonyl derivative $[(\eta^5\text{-}C_5H_5)Ti(Mo_5O_{18})Mn(CO)_3]^{2-}$.

Anion **1** reacts with 2 equiv of aqueous HCl in CH_3CN solution to yield a product which, after recrystallization from $CH_2Cl_2/(C_2H_5)_2O$, analyzes[4] as the $(n\text{-}C_4H_9)_4N^+$ salt of $[(\eta^5\text{-}C_5H_5)Ti\text{-}$

$(\eta^5\text{-}C_5H_5)Ti(Mo_5O_{18})Mn(CO)_3{}^{2-}$
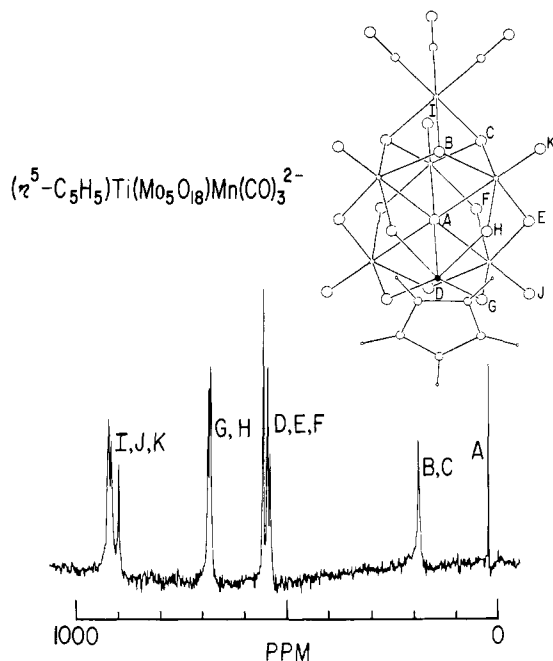
Figure 3. Proposed structure and 13.5-MHz ^{17}O FT NMR spectrum of the C_s $[(\eta^5\text{-}C_5H_5)Ti(Mo_5O_{18})Mn(CO)_3]^{2-}$ anion (**3**). In the structure, one member of each symmetry equivalent set of Mo_5O_{18} oxygens is labeled. Bonds connecting the cyclopentadienyl carbons and the titanium atom (small filled circle) have been omitted for clarity. The spectrum was measured at 77 °C from a 0.1 M CH_3CN solution of the $(n\text{-}C_4H_9)_4N^+$ salt of **3** with all oxygens except the CO oxygens enriched to 20 atom % ^{17}O. Chemical shift values in ppm downfield from pure H_2O: 24 (A), 188 (B, C), 539, 545, 555 (D, E, F), 679, 684 (G, H), 896, 913, 919 (I, J, K).

$(Mo_5O_{18})MoO_2Cl]^{2-}$ (**2**). This new anion, according to X-ray diffraction results described below, has the structure shown in Figure 2 in which an MoO_2Cl^+ unit is bonded to a triangle of three bridging oxygens in the reactant anion structure. Unfortunately, anion **2** resembles anion **1** in that it is unstable toward water and heat, decomposing in CH_3CN to $Mo_6O_{19}{}^{2-}$. Operating on the hypothesis that this instability arises from the presence of $Mo^{VI}\text{-}Cl$ bonds in the MoO_2Cl^+ groups,[5] we prepared the $Mn(CO)_3^+$ adduct[6] of anion **1**, $[(\eta^5\text{-}C_5H_5)Ti(Mo_5O_{18})Mn(CO)_3]^{2-}$ (**3**),[7a] from anion **1** and $[(OC)_3Mn(NCCH_3)_3][PF_6]$ in CH_3CN. Anion **3** is assigned the structure shown in Figure 3, related to the structure of anion **2** by replacement of its MoO_2Cl^+ group with an $Mn(CO)_3^+$ unit, on the basis of its IR spectrum in the carbonyl region[7b] and ^{17}O NMR spectrum (see Figure 3). The spectral assignments given in Figure 3 were made by using the ^{17}O NMR chemical shifts for anion **1** reported in ref 2. Note that the resonances for all OMo, OMo_2, and OMoTi oxygens in anion **3** lie downfield relative to the corresponding resonances in anion **1**. This downfield shift of all pertinent resonances indicates a reduction in charge on the corresponding oxygens over the *entire* $Mo_5O_{18}{}^{5-}$ moiety in **1** upon $Mn(CO)_3^+$ addition.[8]

In contrast with anions **1** and **2**, anion **3** is relatively stable toward both water and heat in CH_3CN. This observation and

(4) Anal. Calcd for $C_{37}H_{77}ClMo_6N_2TiO_{20}$: C, 29.06; H, 5.08; Cl, 2.32; Mo, 37.65; N, 1.83; Ti, 3.13. Found: C, 29.09; H, 5.14; Cl, 2.22; Mo, 37.79; N, 1.82; Ti, 3.25.

(5) Molybdenum(VI) oxochlorides are hydrolytically stable only under strongly acidic conditions: Kepert, D. L. "The Early Transition Metals"; Academic Press: New York, 1972; pp 274–284.

(6) The $Mn(CO)_3^+$ cation has been shown to form a heat and water stable hexametalate complex, $[(OC)_3Mn(Nb_2W_4O_{19})]^{3-}$: Besecker, C. J.; Klemperer, W. G. *J. Am. Chem. Soc.* **1980**, *102*, 7598.

(7) (a) Anal. Calcd for $C_{40}H_{77}MnMo_5N_2TiO_{21}$: C, 31.93; H, 5.16; Mn, 3.65; Mo, 31.88; N, 1.86; Ti, 3.18. Found: C, 32.16; H, 5.23; Mn, 3.73; Mo, 31.64; N, 2.02; Ti, 3.30. (b) IR (CH_3CN, 1850–2050 cm^{-1}): 1924 (br s), 2025 (s).

(8) The response of ^{17}O NMR chemical shifts to charge redistribution in polyoxoanions has been discussed elsewhere: Klemperer, W. G.; Shum, W. *J. Am. Chem. Soc.* **1978**, *100*, 4891.

the similar stability of $VMo_5O_{19}^{3-}$ toward water and heat suggest that the instability of anion **1** may arise in part from relatively high negative charge density on the surface of its $Mo_5O_{18}^{6-}$ subunit. Apparently the $[(C_5H_5)Ti^{IV}]^{3+}$ group, containing a tetravalent metal center, cannot withdraw negative charge from the $Mo_5O_{18}^{6-}$ unit as effectively as the $[OV^V]^{3+}$ group which employs a pentavalent metal center.[9] The negative charge density on the $Mo_5O_{18}^{6-}$ unit in anion **1** can be lowered by addition of an $Mn(CO)_3^+$ unit, resulting in a hydrolytically stable adduct, anion **3**. The mechanism by which charge reduction occurs throughout the entire anion upon adduct formation is revealed by detailed comparison of the structures of anion **1** and its MoO_2Cl^+ adduct, anion **2**.

Single crystals of the $(n\text{-}C_4H_9)_4N^+$ salts of anions **1** and **2**, obtained in the form of their CH_2Cl_2 solvates from $CH_2Cl_2/(C_2H_5)_2O$ solution, were utilized for single-crystal X-ray diffraction structure determinations.[10] Anion **1** (see Figure 1) is structurally related to the $Mo_6O_{19}^{2-}$ anion by substitution of a $[(C_5H_5)Ti^{IV}]^{3+}$ group for an $[OMo^{VI}]^{4+}$ unit. The $Mo_6O_{19}^{2-}$ structure has been shown to approximate full O_h symmetry in the solid state,[11] with small but statistically significant differences in Mo–O bond lengths constituting the major departures from idealized symmetry. Replacement of a $[OMo^{VI}]^{4+}$ unit in $Mo_6O_{19}^{2-}$ by a $[(C_5H_5)Ti^{IV}]^{3+}$ group to give **1** necessarily reduces the anion symmetry and has a pronounced structural effect on the $Mo_5O_{18}^{6-}$ moiety. Similar distortions are observed in $Na_6H_2[Ce(W_5O_{18})_2]\cdot30H_2O$.[12] Even though **1** is not required to possess any rigorous crystallographic symmetry, it approximates rather closely C_{4v} site symmetry (if the local symmetry of the C_5H_5 ring is ignored), with O_E, Mo_5, O_A, Ti, and the cyclopentadienyl center of gravity ideally lying on the fourfold axis. The $[(\eta^5\text{-}C_5H_5)Ti(Mo_5O_{18})MoO_2Cl]^{2-}$ anion (**2**) (see Figure 2) can be derived from **1** by bonding an MoO_2Cl^+ unit to three of its doubly bridging oxygens. Although such a species could ideally approximate C_s-m symmetry if the Cl atom was located in the pseudo mirror plane of **2** determined by Ti, Mo_5, Mo_6, O_A, O_{B1}, O_{B3}, O_E, and the cyclopentadienyl center of gravity, one of the oxygen atoms (O_{G1}) lies in this plane instead. Since the Mo_6–O_{G2} bond has multiple bond character while the Mo_6–Cl bond does not, the symmetrical bonding patterns observed in **1** will be perturbed, with those bonds closest to Mo_6 being affected the most. The bonds to the six atoms closest to each molybdenum in **2** show the normal trends of long bonds being trans to short bonds. Thus the Mo_6–O_{C1} bond length is more than 0.24 Å shorter than Mo_6–O_{C2} [2.021 (8) vs. 2.263 (8) Å]. These large differences in Mo_6–O_C bonds would be expected to affect the remaining two Mo–O_{C2} bonds relative to the remaining Mo–O_{C1} bonds. Thus Mo_5–O_{C1} is more than 0.10 Å longer than Mo_5–O_{C2}

[2.083 (7) vs. 1.982 (8) Å] and Mo_1–O_{C1} is more than 0.06 Å longer than Mo_2–O_{C2} [2.107 (8) vs. 2.037 (9) Å]. As one progresses further from Mo_6, the distortion in bonding parameters from idealized C_s-m symmetry is much less pronounced. Nonetheless, a systematic pattern of trans bond length alternation at molybdenum is observed for sequences of bonds to the doubly bridging OMo_2 oxygen atoms. For the O_B-type oxygens the following sequence of bond lengths, averaged in accord with approximate C_s-m symmetry, is observed: O_{B1}–Mo_2, 2.014 (7,1,1,2) Å;[13] Mo_2–O_{B2}, 1.870 (8,7,7,2) Å; O_{B2}–Mo_3, 1.971 (8,15,15,2) Å; and Mo_3–O_{B3}, 1.919 (8,6,6,2) Å. Analogous considerations apply to bonding at O_{C3} and O_{C4}. Note, however, that bond alternation is *not* observed at titanium.

Acknowledgment. W.G.K. acknowledges the National Science Foundation for support of this research.

Supplementary Material Available: Tables of atomic positional and thermal parameters (10 pages). Ordering information is given on any current masthead page.

(13) The first number in parentheses following an averaged value of a bond length or angle is the root-mean-square estimated standard deviation of an individual datum. The second the third numbers, when given, are the average and maximum deviations from the averaged values, respectively. The fourth number represents the number of individual measurements which are included in the average value.

The First General Index of Molecular Complexity

Steven H. Bertz

*Bell Laboratories,
Murray Hill, New Jersey 07974*

Synthetic chemists have been defining a "complex molecule" in the way that many people define art: they know it when they see it. While the features which contribute to the complexity of a molecule have been discussed,[1-4] no unified index has been formulated which takes into account the size, symmetry, branching, rings, multiple bonds, and heteroatoms characteristic of a complex molecule. This communication shows how concepts from graph theory and information theory can be combined to create the first general index of molecular complexity.

A molecule is commonly represented by its *skeletal molecular graph*, M', (mathematically,[5] the union of a set of points, symbolizing atoms other than hydrogen, and a set of lines, symbolizing bonds). Its properties can then be expressed in terms of *graph-theoretical invariants*, N_{ij}, which Gordon has defined as "the number of distinct ways in which skeleton i can be cut out of skeleton j".[6] The simplest such invariant which takes into account both points and lines is N_{2j}, the number of ways that propane can be cut out of a saturated hydrocarbon, which has been used successfully as a branching index. A more general approach which can be extended to unsaturated systems is based upon η, the number of *connections*, defined as the number of pairs of adjacent lines. For a saturated hydrocarbon, the number of connections equals N_{2j}. Thus, ethane has no connections; propane has one; isobutane, three; and neopentane, six.

In order to include multiple bonds in this scheme, it is necessary to show how "pairs of adjacent lines" are counted in a *multigraph* (a graph with more than one line connecting a pair of points).

(9) The ^{17}O NMR data reported in ref 2 also indicate more negative charge on OMo and OMo_2 oxygens in anion **1** relative to the corresponding oxygens in $VMo_5O_{19}^{3-}$.

(10) Space group and unit cell data for the two compounds are as follows: tetragonal, space group $I4_1cd$-C_{4v}^{12} (no. 110) with $a = b = 25.162$ (9), $c = 50.380$ (10) Å; $Z = 4$ for **1**; monoclinic, space group $P2_1/c$-C_{2h}^5 (no. 14) with $a = 22.871$ (4), $b = 11.942$ (5), $c = 25.127$ (8) Å; $\beta = 110.52$ (3)°; $Z = 4$ for **2**. Intensity measurements were made on a computer-controlled Nicolet PĪ autodiffractometer for both compounds using full (0.90° wide) ω scans and graphite-monochromated Mo Kα radiation. Totals of 7412 (**1**) and 11777 (**2**) independent reflections having $2\theta_{MoK\bar{\alpha}} < 50.70°$ (the equivalent of 0.80 limiting Cu Kα spheres) were measured for both compounds. The titanium and molybdenum atoms of both totally general-position asymmetric units were located by using direct methods (MULTAN); the remaining anionic, cationic, and solvent nonhydrogen atoms were located by standard difference Fourier techniques. The resulting parameters have been refined to convergence [R_1 (unweighted, based on F) = 0.064 for 2556 reflections of **1** having $2\theta_{MoK\bar{\alpha}} < 43°$ and $I > 3\sigma(I)$; $R_1 = 0.057$ for 6882 reflections of **2** having $2\theta_{MoK\bar{\alpha}} < 50.70°$ and $I > 3\sigma(I)$]. Cycles of unit-weighted full-matrix least-squares refinement for both compounds utilized anisotropic thermal parameters for all anionic and solvent nonhydrogen atoms and isotropic thermal parameters for all cationic nonhydrogen atoms. Refinement is continuing for both compounds with the more complete data sets and/or models which incorporate anisotropic thermal parameters for all nonhydrogen atoms.

(11) (a) Allcock, H. R.; Bissel, E. C.; Shawl, E. T. *Inorg. Chem.* **1973**, *12*, 2963. (b) Garner, C. D.; Howlander, N. C.; Mabbs, F. E.; McPhail, A. T.; Miller, R. W.; Onan, K. D. *J. Chem. Soc. Dalton Trans.* **1978**, 1582.

(12) Iball, J.; Low, J. N.; Weakley, T. J. R. *J. Chem. Soc. Dalton Trans.* **1974**, 2021.

(1) Corey, E. J.; *Pure Appl. Chem.* **1967**, *14*, 19–37. *Q. Rev., Chem. Soc.* **1971**, *25*, 455–482.

(2) Hendrickson, J. B. *Top. Curr. Chem.* **1976**, *62*, 49–172.

(3) Woodward, R. B. "Perspectives in Organic Chemistry"; Todd, A., Ed.; Interscience: New York, 1956; p 160. *Pure Appl. Chem.* **1968**, *17*, 519–547.

(4) Ireland, R. E. "Organic Synthesis"; Prentice-Hall: Englewood Cliffs, NJ, 1969; p 100–116.

(5) Harary, F. "Graph Theory"; Addison-Wesley: Reading, MA, 1969. The symbol M is reserved for the full molecular graph, including hydrogen.

(6) Gordon, M.; Kennedy, J. W. *J. Chem. Soc., Faraday Trans. 2* **1973**, *69*, 484–504.